JOURNAL OF VIROLOGY, Jan. 1994, p. 223–232
0022-538X/94/$04.00+0

Vol. 68, No. 1

Electron Microscopy of the Nucleocapsid from Disrupted Moloney Murine Leukemia Virus and of Associated Type VI Collagen-Like Filaments

JEANNE PAGER,† DOMINIQUE COULAUD, AND ETIENNE DELAIN*

Laboratoire de Microscopie Cellulaire et Moléculaire, URA 147 du Centre National de la Recherche Scientifique, Institut Gustave Roussy, F-94805 Villejuif Cedex, France

Received 28 June 1993/Accepted 22 September 1993

To analyze the constituents of retroviruses, the Moloney murine leukemia virus was disrupted and observed by dark-field electron microscopy. Virus disruption was achieved by several methods: osmotic shock, freezing-thawing cycles, and exposure to urea up to 4 M, to NaCl up to 1 M, and to Triton X-100. Several components associated with broken Moloney murine leukemia virus were repeatedly found in preparations. These components have been described as rings, thick filaments, chain-like filaments, threads covered with proteins, threads with buckles, and naked threads. A quantitative analysis of the occurrence of these components has been carried out. Among them, the thick filaments composed of a compact helical arrangement of small beads 5 nm in diameter were considered to represent the nucleocapsid. The protease-sensitive buckles found on some threads could be a compact form of the viral RNA associated to the nucleocapsid protein NCp10. The RNase-sensitive naked threads are interpreted as the deproteinized viral RNA itself. The ubiquitous chain-like filaments possess a periodic structure identical to that of polymerized type VI collagen. It is proposed that this adhesive protein is associated with the viral envelope taken from the cell membrane during the budding process of retroviruses.

The criteria for the classification of *Retroviridae* have been listed in a recent review emphasizing the major contribution of morphology to knowledge on the family (18). The viruses to be studied (Moloney murine leukemia virus [MoMuLV]) or mentioned (Friend murine leukemia virus [FMuLV] and human spumaretrovirus [HSRV]) in this article belong to the subfamily of *Oncovirinae*, in which the assembly and budding, which carry away a portion of the host cell membrane, are observed simultaneously, or to that of *Spumaretroviridae*, in which the two processes are dissociated. In members of the *Retroviridae*, the viral envelope, with an inner coat just beneath it, surrounds the icosahedral outer shell made of hexagonally arranged subunits, within which lies the electron-dense ribonucleoprotein complex, usually considered to form a filamentous spiral (4), although totally convincing images are still lacking. These elements and the viral enzymes (reverse transcriptase, integrase, and protease), each one with a specific molecular weight, are the distinguishing features of the group, but there are variations in the length of the retrovirus genomic RNA, between 7 and 11 kb depending on the virus type. Long after the pioneering electron microscopic (EM) observations of the genome of various retroviruses (17, 23, 29, 31, 35, 41; reviewed in reference 10), it was shown by EM to be a symmetrical linear dimer, joined by a specific dimer linkage structure close to the 5′ ends and bearing one loop, several hairpins, and a poly(A) tail on each strand (3, 33). However, images of purified RNA, denaturated for EM observation, even combined with biochemical results on the genome structure, do not permit us to predict the spatial organization of the genome inside the viral particle.

Although a considerable amount of progress has been achieved on the knowledge on viral constituents (6, 20), it should be noted that EM of isolated viruses has not afforded a clear description of the architecture of the different elements and that the anatomy of these important pathogenic agents needs to be further investigated.

Through our experience in virus disruption (29, 39) and in the use of nonconventional EM imaging modes for the observation of nucleic acid-protein complexes (9, 30), we have been able to visualize the components released by different retroviruses, mainly the MoMuLV, and thus provide a better description of their organization.

MATERIALS AND METHODS

Viruses. MoMuLV particles were harvested from culture supernatants of chronically infected NIH 3T3 fibroblasts. The virus production by cells and the canonical morphology of the virions were checked by EM observation of the viruses retained by a 0.1-μm-pore-size Millipore filter (2). The viral pellet obtained from clarified medium was further purified on a 15 to 60% sucrose gradient. The viral band, with a density of 1.15 g/ml, was collected, diluted, and further centrifuged (116,000 × *g*) for 20 min at 4°C to wash the saccharose away. The final pellet, maintained on ice, was resuspended either in TEN buffer (Tris hydrochloride, 10 mM [pH 7.5]; EDTA, 1 mM; sodium chloride, 100 mM) or in the freezing medium and immediately either used or frozen with 1% saccharose (wt/vol) and kept at −70°C. Unless otherwise mentioned, the suspension and dilution medium was TEN. A fresh sample of FMuLV was purified and processed for EM as for MoMuLV. Twenty milliliters of frozen culture medium containing HSRV harvested from glioblastoma cells was kindly provided by Georges Peries (Saint-Louis Hospital, Paris, France); the infectious

* Corresponding author. Mailing address: Laboratoire de Microscopie cellulaire et moléculaire, Institut Gustave Roussy, Rue Camille Desmoulins, F-94805 Villejuif Cedex, France. Phone: 33 1 45 59 48 76. Fax: 33 1 47 28 92 74.

† Present address: Centre de Biophysique Moléculaire CNRS, F-45071 Orléans Cedex 2, France.

medium was thawed, clarified, and ultracentrifuged on a 20% glycerol cushion before processing for EM.

Viral disruption. The viral disruption methods were adapted from those classically used in viral core preparation: (i) For freezing-thawing cycles, viral samples (1 μl) were alternatively frozen at −20°C and thawed on ice five times, the viral stock being diluted 100 times for EM observation. (ii) For increasing ionic strength, thawed viruses were maintained on ice and submitted to successive 5-min steps of increasing sodium chloride concentration. Molarity was gradually incremented by 100 mM steps, to reach a final concentration of 100 to 1,000 mM. For EM observation, samples were diluted in TEN with the same sodium concentration, maintained on ice for 1 h, and adsorbed onto carbon-coated grids. In some cases, the concentrated virus suspensions incubated in 400 mM NaCl were rapidly diluted in buffer, leading to an osmotic shock which produced a clear visualization of some inner constituents of the virus. (iii) For urea, the same schedule as for ionic strength was applied, with 1 M urea increments, to reach a final concentration of 4 M. (iv) For proteinase K (Merck), freshly harvested viruses were diluted 10 times, digested by 50 μg of proteinase K per ml (1:20 [vol/vol]) for 1 h at 37°C, and set to the final dilution. For chymotrypsin, bovine pancreatic chymotrypsin specially purified by F. Pochon for other purposes (37) was applied to the virus suspension at a concentration of 50 μg/ml for 1 h at 37°C in 20 mM *N*-2-hydroxyethylpiperazine-*N'*-2-ethanesulfonic acid (HEPES)–50 mM NaCl, pH 7.2. (v) For detergents, Triton X-100 (0.04 to 0.1% [vol/vol]) was added to the viral sample for 2 min before the addition of urea (usually 2 M). Fivefold-less concentrated Nonidet P-40 was also tested in combination with urea and provided similar results. So as to limit the superimposition of mechanical effects onto those of the denaturating agents, disrupting solutions were mixed with the viral suspensions very gently.

RNase treatment. A frozen-thawed virus suspension was treated for 30 min at 37°C with 5 μg of DNase-free RNase (Boehringer) per ml in 10 mM Tris–5 mM $CaCl_2$, pH 8.0. The RNase activity was assessed by the effective digestion of phage MS2 RNA in 0.8% agarose gel electrophoresis and in EM preparations under conditions similar to those used to observe the MoMuLV.

EM. The control of virus suspensions and some observations were done in bright-field EM on specimens negatively stained with a 2% aqueous uranyl acetate solution. For EM observations of disrupted viruses, 5 μl of the treated viral suspension was deposited onto a carbon-coated 600-mesh grid activated by glow-discharge in the presence of pentylamine (13). Grids were left for 1 min and washed with 3 drops of aqueous 2% uranyl acetate, dried, and then observed by annular dark-field EM in a Zeiss 902 electron microscope, with inelastically scattered electrons being filtered out to enhance contrast (30). Some negatively stained samples were observed by electron spectroscopic imaging (ESI) with inelastically scattered electrons with a $\Delta E = 114$ eV energy loss, which corresponds to the strong $O_{4,5}$ peak of uranium (9).

Morphometry. In the experiments of viral disruption, the distribution of the various elements was determined systematically, by direct counting on the grids during EM observation. According to the concentration of material deposited on the carbon, 5 to 10 hexagonal windows per grid were randomly chosen for counting in each experimental situation. All the elements were identified and allotted to one of the following classes: intact viruses, broken viruses, rings, protein-covered threads, thick filaments, chain-like filaments, buckled threads, and naked threads. More than 1,500, and often nearly 2,000, elements were considered for each concentration of urea and NaCl. The sample size was close to 1,000 elements in the experiments with Triton X-100. Increasing the sample size further did not modify the overall distribution profiles, but the heterogeneity of composition from one grid window to the other introduced a strong bias in variance analysis, and the distribution of the elements was more accurately compared with one another by using nonparametric statistics (Spearman correlation and Mann-Whitney U test).

The dimensions of elements (width and length), were measured on photographs, either manually or with a PC-driven digitizer. The data are expressed as mean values and confidence intervals with a 5% probability threshold, together with the sample size.

RESULTS

Structural observations. (i) Control of the virus suspension. The purity of the viral suspension was assessed by the absence of cellular debris or other contaminants like mycoplasmas, yeast cells, or bacteria. On negatively stained control preparations, the viruses penetrated by stain displayed a classical morphology (Fig. 1b).

(ii) Dark-field EM observation of the viral suspension. When a virus preparation as used herein is deposited onto carbon films activated by the method of Dubochet et al. (13), used for adsorbing nucleic acid molecules, intact viruses appear as clear spots surrounded by a less-dense round puddle (Fig. 1a, mainly on the left top). Disrupted viruses are present with a larger and irregular puddle of material surrounding a dense body (Fig. 1a, mainly on the right lower part). In addition, various structures, apart from viral remnants, can be seen free in the background. They often consist of short, thick filaments (thin arrows) or chains made of long, thin filaments with very regularly spaced thickenings (thick arrow). In some cases, a more complex organization with various structures connected to the disrupted virus can be observed, such as described in the legend to Fig. 1c.

All these structures are illustrated in the figures, and their dimensions are given below. Since they were found in different proportions in all preparations according to the disruptive conditions, a statistical analysis of their frequency will be presented later. The most typical images were selected for the qualitative analysis, without paying any systematic attention to the disruption procedure used in each case.

FIG. 1. (a) Large field of a frozen-thawed suspension of viruses positively stained and observed in dark-field EM. The undisrupted virions appear as a dense spot surrounded by a puddle of less-dense material; broken virions exhibit a complex patch of material. Two short, dense filaments (thin arrows) and one chain-like filament looking like type VI collagen polymers (thick arrow) are also found in the background. (b) Bright-field EM of a negatively stained virion, in which the stain has penetrated, revealing the inner components. (c) Example of the coexistence, on a single broken virus, of the dense central material of a type VI collagen-like filament and of thin threads with buckles (arrows) described in the legend to Fig. 3. (d) Ring-like objects with a relatively uniform contour length observed in Triton X-100–urea-treated samples, inside of a puddle of faintly stained material (interpreted as remnants of the virus envelope). Most of them present a dense spot(s), which seems to make them circular, compared with a few which are linear. Some smaller rings are also present. (e) High magnification of a ring, with two dense dots and several thin, entangled filaments. Bars, 1 μm (a and d) and 0.1 μm (b, c, and e).

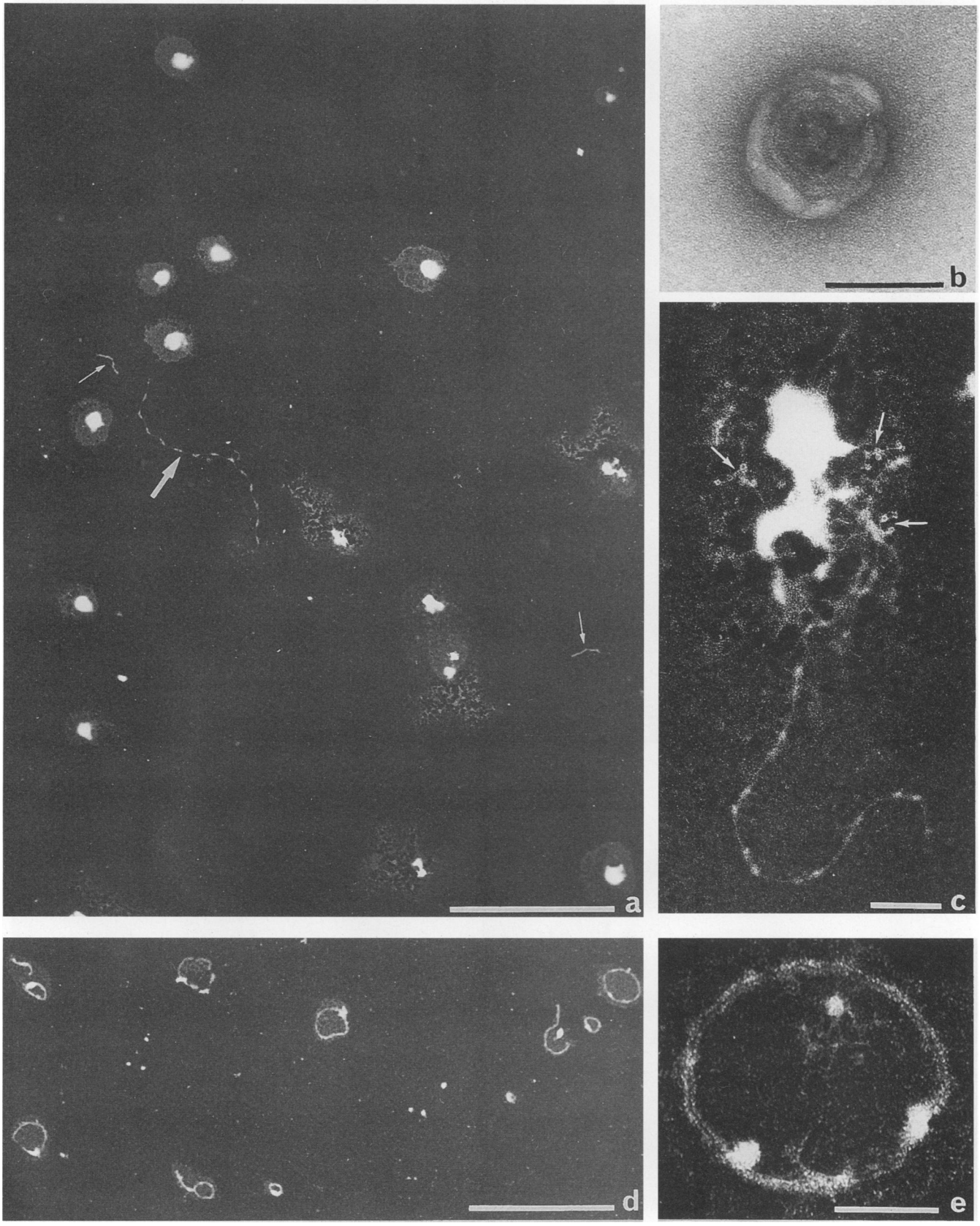

FIG. 1.

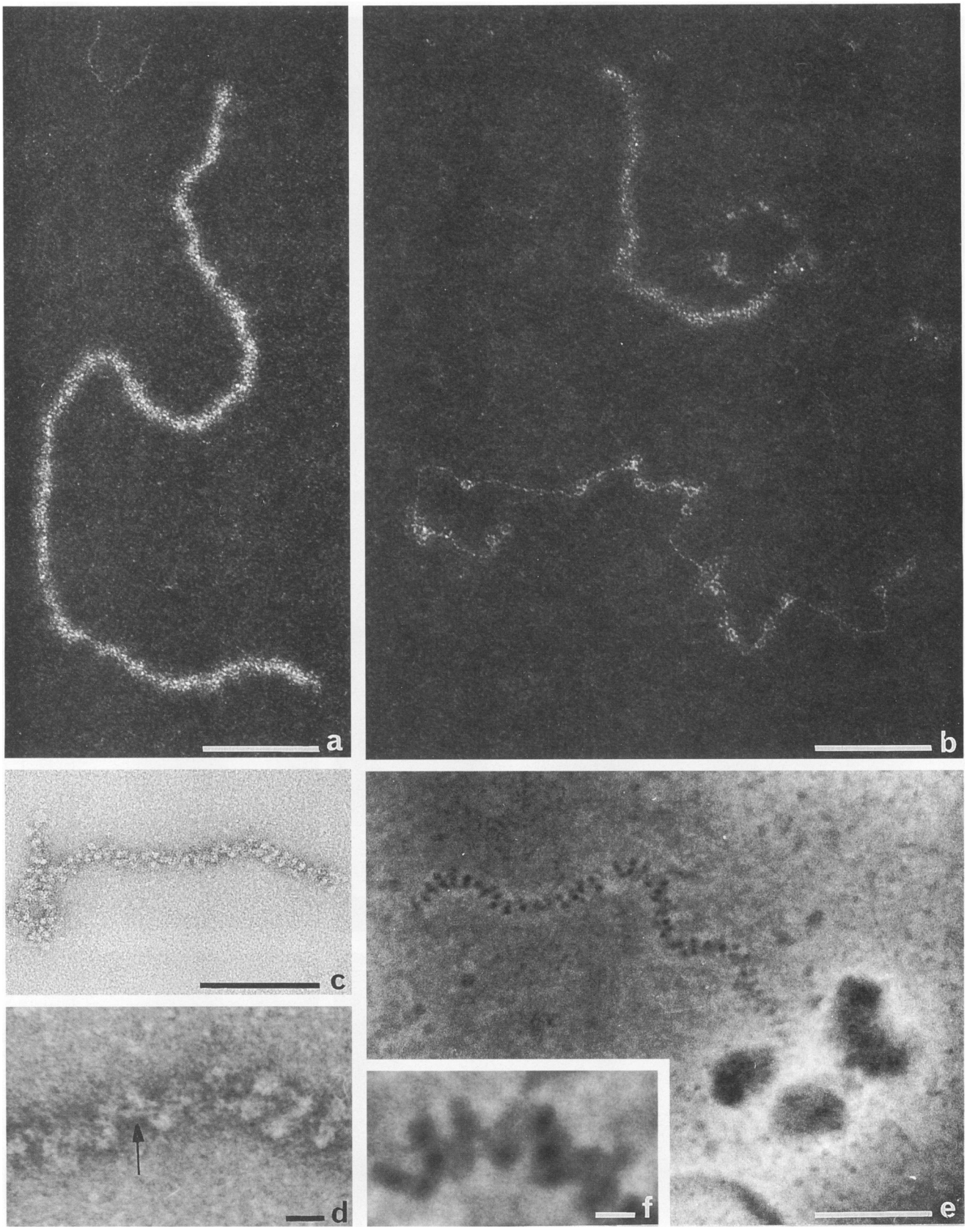

FIG. 2.

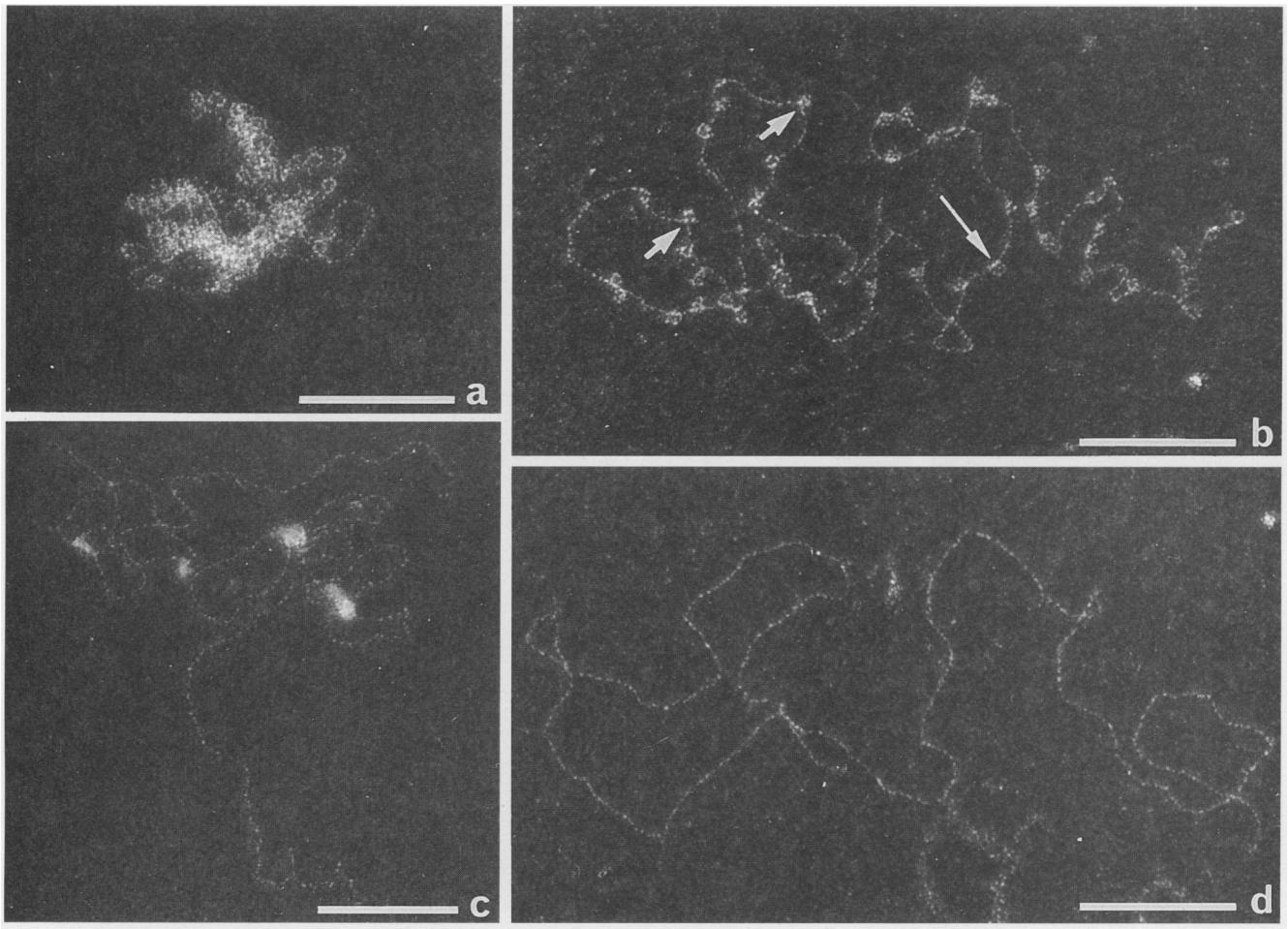

FIG. 3. Filaments with more or less densely packed buckles. (a) Untreated viral suspension; (b) proteinase K-treated viruses. These buckles form different types of loops (arrows), depending on the angle made by the two filaments going in and out of the buckle (see details in the text). (c) Thin, entangled thread with patches of various sizes, considered to be remnant proteins; (d) naked thread (from proteinase K-treated samples). Bars, 0.1 μm.

(iii) Ring-like structures. Annular objects are very frequent in Triton X-100- plus urea-treated samples (Fig. 1d and e). They consist of a ring seemingly composed of two parallel elements, usually bearing one and sometimes several dense dots, and covered with, or locally connected to, irregular patches of dense material.

(iv) Thick filaments. Thick, linear filaments are observed in all preparations and were frequent after NaCl disruption. In positively stained preparations, the filaments have the aspect shown in Fig. 2a. In proteinase K-treated virus suspensions, the thick filaments were often less contrasted (Fig. 2b, top) and were frequently found with the buckled threads described in the legend to Fig. 3 (Fig. 2b, bottom). In negatively stained preparations of NaCl-treated viruses, thick filaments were frequent and seemed to be made of a dense packing of small spheres, about 5 nm in diameter (Fig. 2c). Higher magnification revealed that these spheres could actually be the projection image of a 4.7-nm-wide, probably left-handed, helical filament (Fig. 2d). A thin, straight filament about 1.5 nm wide could be seen in the axis of some loosely packed zones (Fig. 2d, arrow). This helical organization, which made it difficult to measure the actual width of the filaments accurately, is revealed by a zig-zag pattern, clearly visible in preparations observed in the dark-field mode obtained by ESI (Fig. 2e and f).

(v) Threads with buckles. Another typical structure found in

FIG. 2. (a and b) Dark-field EM image of positively stained thick filaments from frozen-thawed (four times) viruses treated with 2 M urea (a) and from proteinase K-treated viruses (b). The thick filament in panel b is altered and less dense than that visible in panel a; it displays some substructures which could be compared to the buckles present on the buckled thread below it (see also Fig. 3). (c to f) Negatively stained thick filaments from an untreated viral suspension (c and d) or from a viral suspension in 1 M NaCl diluted to 1/3 with water on the EM grids (e and f). (c) The filament observed in bright-field EM shows a compact beaded structure and an apparent width similar to that of positively stained thick filaments (panels a and c are at the same magnification). (d) High magnification of a portion of panel c showing the structure of the (possibly left-handed) helically wound 4.7-nm filament and a 1.5-nm-wide central axis (arrow). (e and f) Dark-field ESI of a similar thick filament protruding from a broken virion and showing its helical arrangement (panel f is an enlargement of the central part of the thick filament from panel e). Bars, 0.1 μm (a to c and e) and 10 nm (d and f).

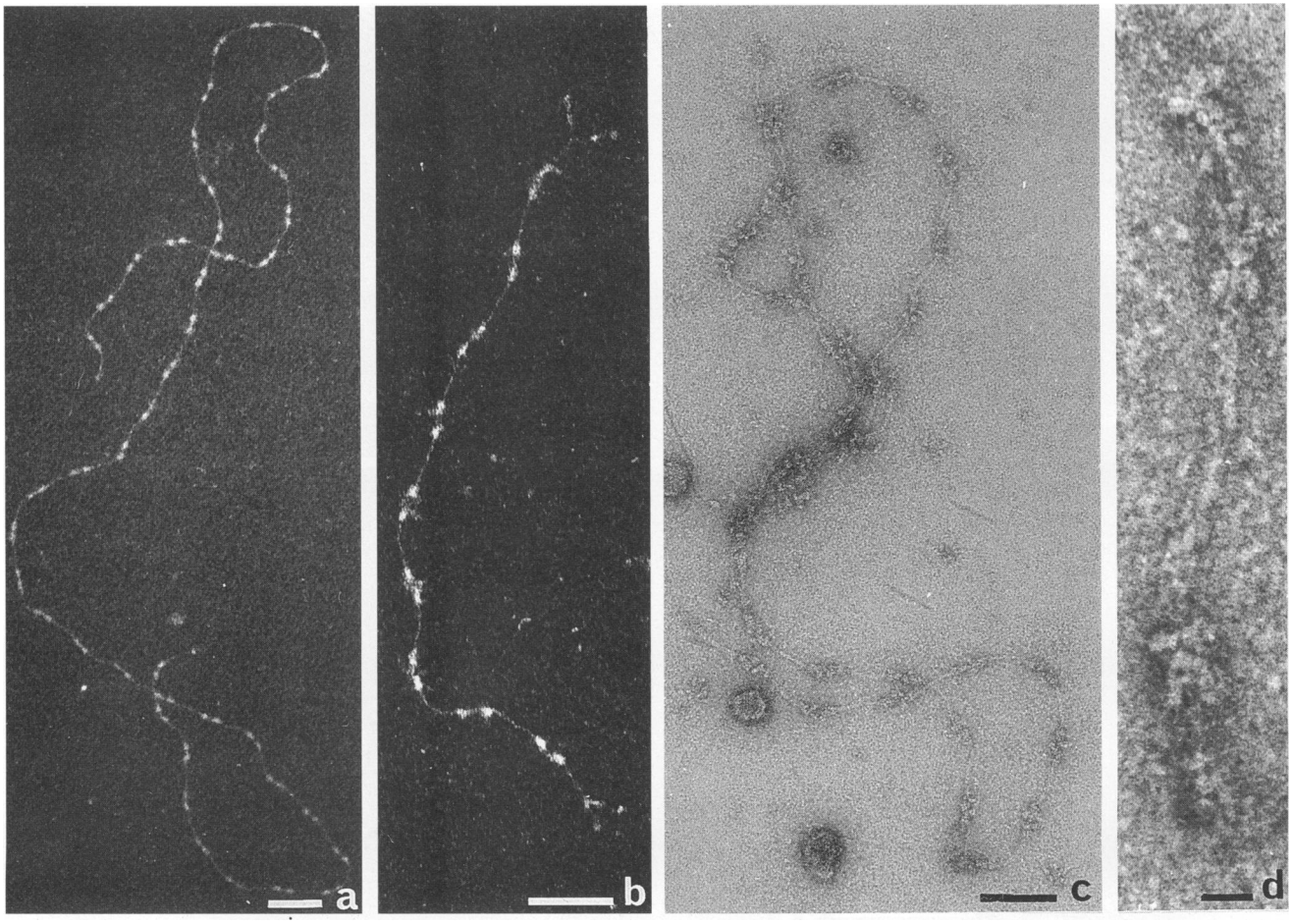

FIG. 4. Type VI collagen-like filaments made of a varied number of elements are found in all types of preparations. The beads found on the polymer are varied in appearance and sizes, depending on the disruption treatment. (a) Five freezing-thawing cycles; (b) rapid dilution in water of the viruses suspended in 1 M NaCl; (c) untreated viral suspension. (b) In some cases, at the end of the long chains, the dimers which constitute the basic pattern are dissociated, as already shown in reference 48. (a and b) Dark-field EM of positively stained preparation; (c and d) bright-field EM of negatively stained preparations. Bars, 0.1 μm (a to c) and 10 nm (d).

the disrupted virus preparations consisted of long, more or less compact, thin threads with small loops or buckles. In the highly densely packed ones, mainly found in either untreated or mildly treated (e.g., 300 mM NaCl) virus preparations, it was rather difficult to distinguish the individual buckles and the thread (Fig. 3a). Their resolution is easier when they are not compact, as is the case when NaCl concentration is higher (400 mM) (Fig. 3b) or after proteinase K treatment. In still higher concentrations of NaCl or 2 M urea, threads with buckles were rarely found. In the buckles, the filament often entered and exited along the same axis (Fig. 3b, long arrows). Rarely, the in and out positions were close to each other, forming a sharp bend or kink in the filament path (Fig. 3b, short arrows). Our contrasting and observation procedures did not reveal any significant density inside the loop. No regular loop pattern could be observed along the threads. Attempts to visualize these buckled threads by negative staining were unsuccessful. It is likely that their fineness was not compatible with this visualization procedure, because of the heavy background often found in the preparations in which they were more frequently observed.

(vi) Proteinated threads. Very thin entangled threads are found in all disrupted virus preparations (Fig. 3c). They often appear to be associated with more or less dense material, considered to be remnant proteins. A precise depiction of their organization was not possible because of the variety of figures formed by these threads.

(vii) Naked threads. Naked threads with a more or less entangled aspect were found preferably when the viruses were submitted to strong treatments: 2 M urea, 500 mM NaCl, or proteinase K (Fig. 3d).

(viii) Collagen-type VI-like filaments. In all the preparations of disrupted viruses, chains or a string of pearls were systematically found, either free or together with virus remnants (Fig. 4). They consisted of long filamentous linear and straight structures of various length, up to several micrometers, about 3 nm wide, regularly covered with patches made of pairs of dense granules, as seen in dark-field EM on positively stained specimens. These pairs of granules were very regular in size in a given sample, and their disposition all along each filament, as well as the distance between two patches, was even more constant, with a periodicity of 110 ± 0.7 nm (86 measurements).

(ix) Enzymatic treatments. In frozen-thawed suspensions of MoMuLV treated with DNase-free RNase, rings, thick filaments, and collagen-like filaments were preserved when all the

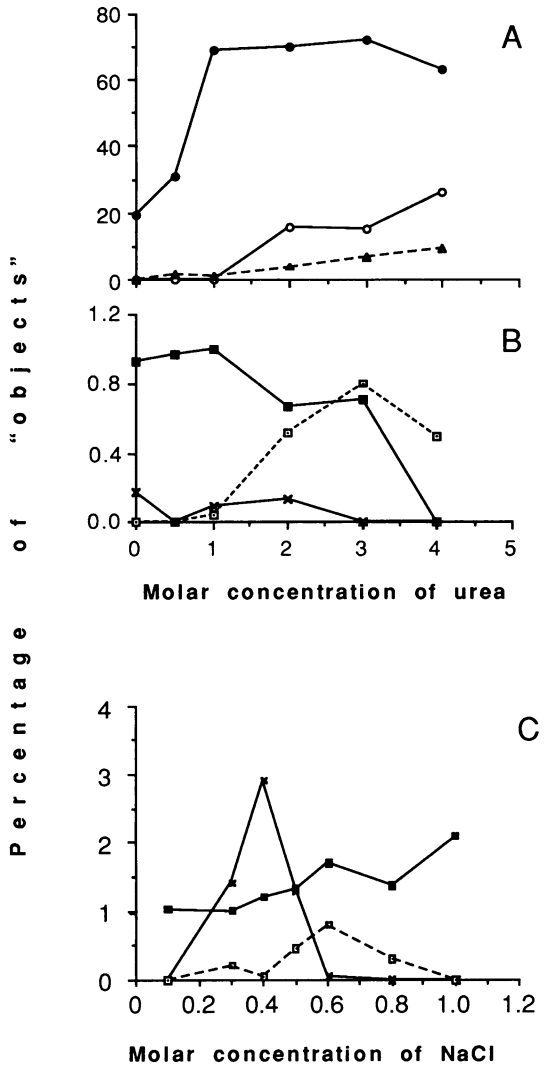

FIG. 5. (A and B) Quantitative distribution of the elements found in the preparation of urea-treated virus suspensions. (A) Major elements: ●, broken viruses; ○, filaments associated with densities (protein remnants); ▲, ring-like structures. When the proportion of disrupted virus increases with the urea concentration, that of ring-like structures and entangled filaments also increases regularly. (B) Minor elements: ■, thick filaments; ⊡, naked threads; ×, threads with buckles. All these elements are relatively sensitive to urea and progressively decrease in frequency with urea concentration. (C) Threads with buckles in the maximum amount (×) are seen at 0.4 M and disappear at 0.6 M NaCl, whereas the naked threads (⊡) are especially found at 0.6 M and disappear at higher sodium concentrations. In contrast, the thick filaments (■) appear progressively with increasing concentration of sodium and were stable at all concentrations.

thin, naked, entangled, or buckled thread-like structures could no longer be found in EM preparations.

In proteinase K-treated preparations, the thick filaments were often less contrasted, and the proportion of buckled threads (4%) was the greatest which could be observed. After a similar treatment with chymotrypsin, rings, thick filaments, and thin threads were conserved, whereas buckles were hardly visible and collagen-like filaments were no longer detectable.

Distribution of the various structures. The structures found in disrupted virus preparations were observed systematically, but their relative distribution depended on the treatment. These distributions related to urea, and some of those related to NaCl treatment are presented in Fig. 5. It has to be noted first that control preparations without any treatment had been frozen and thawed once and then contained 20% broken viruses and about 1% thick filaments. The occurrence of disrupted viruses reached a 70% plateau at 1 M urea, while that of rings and protein-associated threads increased regularly with the urea concentration (Fig. 5A). The proportion of naked threads also increased, seemingly at the expenses of thick filaments, while the occurrence of threads with buckles did not vary significantly according to urea concentration (Fig. 5B).

Although the dose-effect curves were less regular with increasing NaCl than with urea, several similarities can be underlined. The same maximal percentage of disrupted viruses could be reached for 0.6 to 0.8 M NaCl and was decreased beyond, as it was the case for the highest values of urea or Triton X-100, which probably destroyed the structures identified as broken viruses into their constituent elements. As with urea, a significant covariance is observed between the occurrences of ring-like elements and of protein-associated threads, and a peak value was reached at 0.2 M NaCl. The maximal occurrence was observed at 0.4 M NaCl for threads with buckles and at 0.6 M for naked threads, while buckles had disappeared, suggesting a transformation of the former structure into the latter one (Fig. 5C). The frequency of thick filaments increased slightly but regularly, from 1 to 2%, at the successive Na^+ increments.

The most conspicuous and specific result obtained with Triton X-100 plus 2 M urea was the striking production of ring-like structures—up to 50% of the elements observed at 0.4 M Triton X-100. The dose-effect curve was exactly the inverted image of that obtained for broken viruses. Neither detergents nor the other disrupting treatments were noted to change noticeably the relative proportion of collagen-like filaments, since their occurrence range was 0.5 to 1% in any experimental situation.

Measurement of the various structures. Systematic measurements of the elements described previously were made on micrographs, either to help identify them or to compare them with better-known structures. For a constant concentration (2 M) of urea, the length of the rings varied from 0.59 ± 0.08 μm (n = 11) in 0.02% Triton X-100 to 0.68 ± 0.06 μm (n = 10) in 0.05% Triton X-100. At the latter concentration, a second population of larger rings could be observed (1.60 ± 0.58 μm; n = 7), with a maximum length of 2 μm. At a given concentration (0.025%) of Triton X-100, the ring size was dependent on urea concentration: 2 M (0.65 ± 0.05 μm; n = 23) or 4 M (0.51 ± 0.06 μm; n = 17).

The width of the thick filaments, as measured on positively stained preparations, was 13.1 ± 0.75 nm (n = 11); their length varied between 0.16 and 1.03 μm (n = 47), with a bimodal distribution (modal sizes: 0.3 μm for the maximum and 0.9 μm for the minimum). Similar measurements were done on negatively stained, 1 M NaCl-treated viruses, broken by disruption with water on the grid; the length distribution was monomodal (mode size = 0.3 μm; n = 74), with the extreme values equal to 0.06 and 0.54 μm. The maximal width was then 14.0 nm.

Buckles associated with thin threads of various length and observed in positively stained samples have a very regular diameter of 6.5 ± 0.04 nm (189 measurements). The length measurements of naked and buckled threads, including the

perimeter of the buckles, presented a clear maximum for lengths between 1.3 and 2.1 μm, and a smaller peak for lengths over 3.3 μm (n = 125). Combination of the length measurements of naked and buckled threads was allowed because both elements alone displayed similar bimodal distributions, with a clear peak at 1.7 μm and a small peak at 3.5 μm. A few filaments reached up to 4 μm.

DISCUSSION

In the present work the components of the MoMuLV have been visualized by EM after the virions were disrupted by various procedures. The absence of biological contaminants in the viral suspensions was assessed regularly. Structurally characteristic elements were observed systematically in all preparations, either merely thawed from the frozen stock or submitted further to disrupting treatments. The same elements were also found in preparations of FMuLV and of HSRV observed as controls; they are thus considered to be integral parts of the viruses, or to be systematically associated with the viral particles. They have been described here for the first time in their present form, thanks to an EM observation method routinely used in our laboratory to visualize free or protein-associated nucleic acids (9, 30).

The heterogeneous sensitivity of viral samples to disrupting agents has been repeatedly underscored and ascribed in murine leukemia viruses to the time elapsing between virus budding and harvesting (31), to viral source (animals or cell cultures) (15), or to viral molecular maturation, especially precursor protein cleavage (17, 52). The latter hypothesis has been confirmed in more recent human immunodeficiency virus studies (22, 25, 27). There is thus little hope to obtain homogeneous populations of viral elements in the preparations of disrupted viruses. Therefore, we have examined the effects of increasing doses of a given breaking agent on the same viral sample. Regarding the temporal kinetics of disruption, we have studied the range between 5 to 60 min of various treatments. It came out that the whole effect was reached at 5 min; shorter time scales were not accessible because of the irreducible spreading duration. Waiting longer than 10 min did not provide further information.

Treatments with detergents, urea, or high NaCl concentrations achieve the total destruction of the viral envelope and dissociate the subunits of the capsid. Urea, known to be a strong protein denaturant, induces the progressive appearance of ring-like structures and that of complex entangled filaments partially covered with proteins, while thick filaments become less numerous. High urea concentrations can also dissociate RNA from the nucleocapsid proteins, which accounts for the increased occurrence of the naked threads interpreted as the viral RNA, since they have disappeared after DNase-free RNase digestion, while they resist proteases. Compounds liberated by virus disruption might be responsible for the unusually good EM visualization of this single-stranded RNA.

It is interesting to note that the overall effects of three freezing-thawing cycles are identical to those of 1.5 M urea. A less drastic breaking effect than with 1 M urea is observed with NaCl at any concentration. The increasing steps of Na^+ concentration seem to successively induce the appearance of the rings and protein-associated thin filaments, the buckles, and finally the naked threads. We think that the various structures reflect different stages of the nucleocapsid disorganization, although we lack decisive protein identification and had to rely partly on comparison with similar structures described for other viruses or other organisms.

Previous studies on negatively stained disrupted retroviruses have disclosed the nucleocapsid as a coiled, elongated body (29, 31). The functional circular ribonucleoprotein complexes isolated from the avian myeloblastosis virus (6) are similar in length, but not in appearence, to our ring-like objects; described as beaded chromatin-like filaments, they seem to be more empasted with proteins than our so-called thick filaments, with no structure as small as our buckles being detectable on their pictures because of their preparation procedure, including chemical fixation and rotary shadowing. The thick filaments (Fig. 3) are comparable in morphology to thick chromatin fibers, but they are one-half as wide (16.5 instead of 30 nm [Fig. 1i from reference 51]) and remain stable at NaCl and urea concentrations known to denature chromatin (45). Their size is close to that of the "filamentous structures of helical symmetry probably representing the ribonucleoprotein of the feline leukemia virus" (about 14 nm [Fig. 11b and c from reference 17]) or that of the influenza virus nucleocapsid (15 nm) (38). A helical arrangement, which can be seen on our images of negatively stained thick filaments, has also been shown in the core, or nucleocapsid, of a retrovirus isolated from HeLa cells (19).

The diameter of small loops or buckled threads (Fig. 4), 6.5 nm as a mean, can be compared with that (5 to 6 nm) of the globular particles described for *Thermoplasma acidophilum* as DNA associated to a histone-like protein (42). Filaments isolated from disrupted Rauscher leukemia virus, interpreted by Luftig and Kilham as the ribonucleoprotein complex, had a 7-nm periodicity (31). In the same conditions of observation as those used here, classical nucleosomes, from the chromatin of the bovine papilloma virus or of eukaryotic cells, measure 8 to 10 nm (7a, 36), while neutron scattering gives 11 nm (1). Buckles, 9 nm in diameter, are also formed when poly(ADP-ribose) polymerase is complexed to DNA (11, 26). It is interesting to note that the diameter of the buckles on RNA strands from disrupted MoMuLV is close to that of the small globular particles observed to form the thick filaments in negatively stained preparations. These buckles are totally destroyed by chymotrypsin; they disappear in 3 M urea and in 1 M NaCl, as classical nucleosomes are known to do (21, 40, 47). They could be formed, as has been suggested by Searcy and Stein (42) on another model, by the association of the viral RNA and NCp10, a nucleocapsid protein known to participate in several steps of the retroviral cycle (12).

Thin threads represent the ultimate components observed after the most denaturing treatments. Being digested by DNase-free RNase, resistant to proteases, and morphologically different from DNA strands observed in the same conditions, they can be reasonably considered as fragments of the genomial RNA. The length distribution, between 0.3 and 4.1 μm and the presence of two modes, the second one located at a length twice as long as the first one (namely, 1.7 and 3.5 μm), are compatible with this interpretation, considering the maximum length which could be ascribed to the 8.3-kb dimer genome (two monomers of 2.3 μm each, taking 0.28 nm for the distance between adjacent bases). Assuming that thick filaments generate buckled and naked threads, the degree of compaction of genomial RNA in the RNA-NCp10 complex of the nucleocapsid can be estimated to about 5, from the ratio of the modal length of thick filaments (0.3 μm) to that of the naked threads (1.7 μm).

Very few molecules with a morphology which could be compared to that of our chain-like filaments have been described in the literature. Multimers of the von Willebrand factor present a periodicity of 120 nm but are far more contorted than the chain-like filaments (8a, 16). However, the RNase resistance, the protease sensitivity, and the strikingly

similar structure and periodicity (110 nm) of type VI collagen polymers (5, 14, 28, 48, 49) compared with those of chain-like filaments leads us to consider these elements as the actual extracellular matrix-associated polymer. A variability in length, similar to that observed here, has been described for type VI collagen, depending on the enzyme used to extract it from the extracellular matrix (14), since long polymers appear to result from an association with hyaluronan (28). An original observation is the constant presence of these collagen-like polymers in our preparations, in MoMuLV, FMuLV, and HSRV, to an amount of 1%, only slightly modulated according to the disrupting conditions. Type VI collagen is ubiquitous in connective tissues (48) and could be synthesized by the NIH 3T3 fibroblasts as an adhesive protein of the cellular matrix taken away with the cell membrane during virus budding. The chain-like filaments were not found in EM controls either of fetal calf serum or of culture supernatants and thus do not seem to be contaminants. They could represent a physiologic witness to the normal relations between viruses and host membranes, as is the case for human immunodeficiency virus and cell surface proteins (50) or for paramyxoviruses and cytoskeletal proteins (8). Some observations (data not shown) suggest that chain-like filaments could participate in the mechanical stability of the viral envelope. Further experiments are now envisaged, firstly to ascertain the nature of the type VI collagen in chain-like filaments, and secondly to determine their localization and function in the virus-cell interactions.

The elements described in this article were also observed when HSRV was disrupted like as were the murine leukemia viruses. In phylogenetic studies of members of *Retroviridae*, MoMuLV appeared to have diverged early from the common trunk (7, 44). From phylogenesis based on the reverse transcriptase sequence of the *pol* gene, HRSV has been shown to evolve probably from murine leukemia viruses by acquiring a regulatory gene (32). Despite the evolutive proximity, members of *Spumaretroviridae* and *Oncornaviridae* are clearly separated from each other, according to morphologic criteria (18). Their similar nucleocapsid organization prompted us to consider that RNA could be compacted similarly in most retroviruses.

The cellular organization of genetic material has led to classify prokaryotes apart from eukaryotes. The genome of archaebacteria, which are now isolated from prokaryotes, is arranged in nucleosome-like particles, each one involving about 130 bp, and even 250 bp in some cases, irrespective of whether they possess histone-like or mere DNA-binding proteins (24, 34, 36, 42, 43, 46). The elaborate folding of RNA in retroviruses might lead us to question their position among the most primitive living organisms, unless this represents a convergence between the host cell and the viral parasite.

ACKNOWLEDGMENTS

Catherine Ropert in our laboratory and Martine Canivet (G. Peries' group) are thanked for providing FMLV and HSRV samples. Numerous discussions took place with B. Révet concerning virus-disrupting conditions, and the competence of R. Garrone and his colleagues helped us to interpret our images of long filamentous type VI collagen-like structures. We express our special appreciation to Lorna Saint-Ange for the extensive and thorough editing of the English version of the manuscript.

REFERENCES

1. **Baldwin, J. P., P. G. Boseley, E. M. Bradbury, and K. Ibel.** 1975. The subunit structure of the eukaryotic chromosome. Nature (London) **253**:245–249.
2. **Barbieri, D., E. Delain, P. Lazar, G. Hue, and G. Barski.** 1970. Method of virus particles counting using Millipore filtration. Virology **42**:544–547.
3. **Bender, W., Y.-S. Chien, S. Chattopadhyay, P. K. Vogt, M. B. Gardner, and N. Davidson.** 1978. High-molecular-weight RNAs of AKR, NZB, and wild mouse viruses and avian reticuloendotheliosis virus all have similar structures. J. Virol. **25**:888–896.
4. **Bolognesi, D. P., R. C. Montelaro, and S. J. Sullivan.** 1977. A model for assembly of type C oncornaviruses. Med. Microbiol. Immunol. **164**:97–113.
5. **Bruns, R. R.** 1984. Beaded filaments and long-spacing fibrils: relation to type VI collagen. J. Ultrastruct. Res. **89**:136–145.
6. **Chen, M.-J., C. F. Garon, and T. S. Papas.** 1980. Native ribonucleoprotein is an efficient transcriptional complex of avian myeloblastosis virus. Proc. Natl. Acad. Sci. USA **77**:1296–1300.
7. **Chiu, I. M., A. Yaniv, J. E. Dahlberg, A. Gazit, S. F. Skuntz, S. R. Tronick, and S. A. Aaronson.** 1985. Nucleotide sequence evidence for relationship of AIDS retrovirus to lentiviruses. Nature (London) **317**:366–368.

7a. **Couland, D., et al.** Unpublished data.

8. **De, B. P., A. L. Burdsall, and A. K. Banerjee.** 1993. Role of cellular actin in human parainfluenza virus type 3 genome transcription. J. Biol. Chem. **268**:5703–5710.

8a. **Delain, E., and S. Chwetzoff.** Unpublished data.

9. **Delain, E., A. Fourcade, B. Révet, and C. Mory.** 1992. New possibilities in the observation of nucleic acids by electron spectroscopic imaging. Microsc. Microanal. Microstruct. **3**:175–186.
10. **Delius, H., P. H. Duesberg, and W. F. Mangel.** 1975. Electron microscope measurements of Rous sarcoma virus RNA. Cold Spring Harbor Symp. Quant. Biol. **39**:835–843.
11. **De Murcia, G., J. Jongstra-Bilen, M.-E. Ittel, P. Mandel, and E. Delain.** 1983. Poly(ADP-ribose) polymerase automodification and interaction with DNA: electron microscopic visualization. EMBO J. **2**:543–548.
12. **De Rocquigny, H., D. Ficheux, C. Gabus, B. Allain, M. C. Fournie-Zaluski, J.-L. Darlix, and B. P. Roques.** 1993. Two short basic sequences surrounding the zinc finger of nucleocapsid protein NCp10 of Moloney murine leukemia virus are critical for RNA annealing activity. Nucleic Acids Res. **21**:823–829.
13. **Dubochet, J., M. Ducommun, M. Zollinger, and E. Kellenberger.** 1971. A new preparation method for dark-field electron microscopy of biomacromolecules. J. Ultrastruct. Res. **35**:147–167.
14. **Engel, J., H. Furthmayr, E. Odermatt, H. von der Mark, M. Aumailley, R. Fleischmajer, and R. Timpl.** 1985. Structure and macromolecular organization of type VI collagen. Ann. N.Y. Acad. Sci. **460**:25–46.
15. **Feller, U., R. M. Dougherty, and H. S. Di Stephano.** 1971. Comparative morphology of avian and murine leukemia viruses. J. Natl. Cancer Inst. **47**:1289–1292.
16. **Fowler, W. E., L. J. Fretto, K. K. Hamilton, H. P. Erickson, and P. A. McKee.** 1985. Substructure of human von Willebrand factor. J. Clin. Invest. **76**:1491–1500.
17. **Frank, H., H. Schwarz, T. Graf, and W. Schäfer.** 1978. Properties of mouse leukemia viruses. XV. Electron microscopic studies on the organization of Friend leukemia virus and other mammalian C-type viruses. Z. Naturforsch. Sect. C **33**:124–138.
18. **Gelderblom, H. R.** 1991. Assembly and morphology of HIV: potential effect of structure on viral function. AIDS **5**:617–638.
19. **Gelderblom, H. R., H. Bauer, H. Ogura, R. Wigand, and A. B. Fischer.** 1974. Detection of oncornavirus-like particles in HeLa cells. I. Fine structure and comparative morphological classification. Int. J. Cancer **13**:246–253.
20. **Gelderblom, H. R., E. H. S. Haussmann, M. Özel, G. Pauli, and M. A. Koch.** 1987. Fine structure of human immunodeficiency virus (HIV) and immunolocalization of structural proteins. Virology **156**:171–176.
21. **Germond, J.-E., M. Bellard, P. Oudet, and P. Chambon.** 1976. Stability of nucleosomes in native and reconstituted chromatins. Nucleic Acids Res. **3**:3173–3192.
22. **Goto, T., K. Ikuta, J. J. Khang, C. Morita, K. Sano, M. Komatsu, H. Fujita, S. Kato, and M. Nakai.** 1990. The budding of defective human immunodeficiency virus type 1 (HIV 1) particles from cell clones persistently infected with HIV 1. Arch. Virol. **111**:87–101.
23. **Granboulan, N., J. Huppert, and F. Lacour.** 1966. Examen au microscope électronique du RNA du virus de la myéloblastose

aviaire. J. Mol. Biol. **16:**571–575.
24. **Griffith, J. D.** 1976. Visualization of procaryotic DNA in a regularly condensed chromatin-like fiber. Proc. Natl. Acad. Sci. USA **73:**563–567.
25. **Höglund, S., L.-G. Öfverstedt, Å. Nilsson, P. Lundquist, H. Gelderblom, M. Özel, and U. Skoglund.** 1992. Spatial visualization of the maturing HIV-1 core and its linkage to the envelope. AIDS Res. Human Retroviruses **8:**1–7.
26. **Ittel, M.-E., J. Jondstra-Bilen, C. Niedergang, P. Mandel, and E. Delain.** 1985. DNA-poly(ADP-ribose) polymerase complex: isolation of the DNA wrapping the enzyme molecule, p. 60–68. *In* F. R. Althaus, H. Hilz, and S. Shall (ed.), ADP-ribosylation of proteins. Springer-Verlag, Berlin.
27. **Katsumoto, T., N. Hattori, and T. Kurimura.** 1987. Maturation of human immunodeficiency virus, strain LAV, *in vitro*. Intervirology **27:**148–153.
28. **Kielty, C. M., S. P. Whittaker, M. E. Grant, and C. A. Shuttleworth.** 1992. Type VI collagen microfibrils: evidence for a structural association with hyaluronan. J. Cell Biol. **118:**979–990.
29. **Lacour, F., A. Fourcade, A. Verger, and E. Delain.** 1970. Coiled structure of the nucleocapsid of avian myeloblastosis virus. J. Gen. Virol. **9:**89–92.
30. **Le Cam, E., B. Théveny, B. Mignotte, B. Révet, and E. Delain.** 1991. Quantitative electron microscopic analysis of DNA-protein interactions. J. Electron Microsc. Techn. **18:**375–386.
31. **Luftig, R. B., and S. S. Kilham.** 1971. An electron microscope study of Rauscher leukemia virus. Virology **46:**277–297.
32. **Maurer, B., and R. H. Flügel.** 1988. Genomic organization of the human Spumaretrovirus and its relation to AIDS and other retroviruses. AIDS Res. Hum. Retroviruses **4:**467–473.
33. **Murti, K. G., M. Bondurant, and A. Tereba.** 1981. Secondary structural features in the 70S RNAs of Moloney murine leukemia and Rous sarcoma virus as observed by electron microscopy. J. Virol. **37:**411–419.
34. **Musgrave, D. R., K. M. Sandman, and J. N. Reeve.** 1991. DNA binding by the archaeal histone HMf results in positive supercoiling. Proc. Natl. Acad. Sci. USA **88:**10397–10401.
35. **Nermut, M. V., H. Frank, and W. Schäfer.** 1972. Properties of mouse leukemia viruses. III. Electron microscopic appearance as revealed after conventional preparation techniques as well as freeze-drying and freeze-etching. Virology **49:**345–358.
36. **Olins, A. L., M. B. Senior, and D. E. Olins.** 1976. Ultrastructural features of chromatin ν bodies. J. Cell Biol. **68:**787–792.
37. **Pochon, F., V. Favaudon, M. Tourbez-Perrin, and J. G. Bieth.** 1981. Localization of the two proteinase binding sites in human α_2-macroglobulin. J. Biol. Chem. **256:**547–550.
38. **Pons, M. W., I. T. Schulze, G. K. Hirst, and R. Hauser.** 1969. Isolation and characterization of the ribonucleoprotein of influenza virus. Virology **39:**250–259.
39. **Révet, B., and E. Delain.** 1982. The *Drosophila* X virus contains a double-stranded RNA circularized by a 67-Kd terminal protein: high-resolution denaturation mapping of its genome. Virology **123:**29–44.
40. **Rhodes, D.** 1985. Structural analysis of a triple complex between the histone octamer, a *Xenopus* gene or 5S RNA and transcription factor IIIA. EMBO J. **4:**3473–3482.
41. **Sarkar, N. H., R. C. Nowinski, and D. H. Moore.** 1971. Helical nucleocapsid structure of the oncogenic ribonucleic acid viruses (oncornaviruses). J. Virol. **8:**564–572.
42. **Searcy, D. G., and D. B. Stein.** 1980. Nucleoprotein subunit structure in an unusual prokaryotic organism: *Thermoplasma acidophilum*. Biochim. Biophys. Acta **609:**180–195.
43. **Shioda, M., K. Sugimori, T. Shiroya, and S. Takayanagi.** 1989. Nucleosomelike structures associated with chromosomes of the archaebacterium *Holobacterium salinarum*. J. Bacteriol. **171:**4514–4517.
44. **Sonigo, P., M. Alizon, K. Staskus, D. Klatzmann, S. Cole, O. Danos, E. Retzel, P. Tiollais, A. Haase, and S. Wain-Hobson.** 1985. Nucleotide sequence of the Visna lentivirus: relationship to the AIDS virus. Cell **42:**369–382.
45. **Thoma, F., T. Koller, and A. Klug.** 1979. Involvment of histone H1 in the organization of the nucleosome and of the salt-dependent superstructures of chromatin. J. Cell Biol. **83:**403–427.
46. **Torres-Guerrero, H., D. A. Peattie, and I. Meza.** 1991. Chromatin organization in *Entamoeba histolytica*. Mol. Biochem. Parasitol. **45:**121–130.
47. **Touchette, N. A., and R. D. Cole.** 1992. Effects of salt concentration and H1 histone removal on the differential scanning calorimetry of nuclei. Biochemistry **31:**1842–1849.
48. **Van der Rest, M., and R. Garrone.** 1991. Collagen family of proteins. FASEB J. **5:**2814–2823.
49. **Von der Mark, H., M. Aumailley, G. Wick, R. Fleischmajer, and R. Timpl.** 1984. Immunocytochemistry, genuine size and tissue localization of collagen VI. Eur. J. Biochem. **142:**493–502.
50. **Weeks, B. S., K. Desai, P. M. Loewenstein, M. E. Klotman, P. E. Klotman, M. Green, and H. K. Kleinman.** 1993. Identification of a novel cell attachment domain in the HIV-1 Tat protein and its 90-kDa cell surface binding protein. J. Biol. Chem. **268:**5279–5284.
51. **Woodcock, C. L., H. Woodcock, and R. A. Horowitz.** 1991. Ultrastructure of chromatin. I. Negative staining of isolated fibers. J. Cell Sci. **99:**99–106.
52. **Yoshinaka, Y., and R. B. Luftig.** 1977. Murine leukemia virus morphogenesis: cleavage of p70 in vitro can be accompanied by a shift from a concentrically coiled internal strand ("immature") to a collapsed ("mature") form of the virus core. Proc. Natl. Acad. Sci. USA **74:**3446–3450.